

Climate effects on vegetation vitality at the treeline of boreal forests of Mongolia

Michael Klinge¹⁾, Choimaa Dulamsuren²⁾, Stefan Erasmi¹⁾, Dirk Nikolaus Karger³⁾, Markus Hauck²⁾

¹⁾ Institute of Geography, University of Goettingen
Goldschmidtstr. 5, D-37077 Goettingen, Germany

²⁾ Albrecht-von-Haller Institute for Plant Sciences
Plant Ecology and Ecosystems Research, University of Goettingen
Untere Karspuele 2, D-37073 Goettingen, Germany

³⁾ Swiss Federal Research Institute WSL, Züricherstrasse 111, 8903 Birmensdorf, Switzerland

Keywords: Boreal forest, remote sensing, climate analysis, vegetation index

Abstract

In northern Mongolia, at the southern boundary of the Siberian boreal forest belt, the distribution of steppe and forest is generally linked to climate and topography, making this region highly sensitive to climate change and human impact. Detailed investigations on the limiting parameters of forest and steppe in different biomes provide necessary information for paleoenvironmental reconstruction and prognosis of potential landscape change. In this study, remote sensing data and gridded climate data were analyzed in order to identify main distribution patterns of forest and steppe in Mongolia and to detect driving environmental factors for forest distribution. Forest distribution and vegetation vitality derived from the normalized differentiated vegetation index (NDVI) were investigated for the three types of boreal forest present in Mongolia (taiga, subtaiga, and forest-steppe), which cover a total area of 73,818 km². In addition to the forest type areas, the analysis focused on subunits of forest and non-forested areas at the upper and lower treeline, which represent ecological borders between vegetation types. Climate and NDVI data were analyzed for a reference period of 15 years from 1999 to 2013.

The presented approach for treeline delineation by identifying representative sites mostly bridges local forest disturbance like fire or tree cutting. Moreover, this procedure provides a valuable tool to distinguish the potential forested area. The upper treeline generally rises from 1,800 m above sea level (a.s.l.) in the northeast to 2,700 m a.s.l. in the south. The lower treeline locally emerges at 1,000 m a.s.l. in the northern taiga and rises southward to 2,500 m a.s.l. The latitudinal gradient of both treelines turns into a longitudinal one on the eastern flank of mountain ranges due to higher aridity caused by rain-shadow effects. Less productive trees in terms of NDVI were identified at both, the upper and lower treeline in relation to the respective total boreal forest type area. The mean growing season temperature (MGST) of 7.9-8.9 °C and a minimum MGST of 6 °C is a limiting parameter at the upper treeline but is negligible for the lower treeline. The minimum of the mean annual precipitation (MAP) of 230-290 mm y⁻¹ is a limiting parameter at the lower treeline but even at the upper treeline in the forest-steppe ecotone. In general, NDVI and MAP are lower in grassland, and MGST is higher compared to the corresponding boreal forest. One exception occurs at the upper treeline of the subtaiga and taiga, where the alpine vegetation consists of mountain meadow mixed with shrubs. The relation between NDVI and climate data corroborates that more precipitation and higher temperatures generally lead to higher greenness in all ecological subunits. MGST is positively correlated with MAP of the total area of forest-steppe, but this correlation turns negative in the taiga. The limiting factor in the forest-steppe is the relative humidity and in the taiga, it is the snow cover distribution. The subtaiga represents an ecological transition zone of approximately 300 mm y⁻¹ precipitation, which occurs independently from the MGST.

45 Since the treelines are mainly determined by climatic parameters, the rapid climate change in Inner
46 Asia will lead to a spatial relocation of tree communities, treelines and boreal forest types. However,
47 a deduction of future tree vitality, forest composition, and biomass trends directly from the recent
48 relationships between NDVI and climate parameters is challenging. Besides human impact, it must
49 consider bio- and geocological issues like e.g. tree rejuvenation, temporal lag of climate adaptation
50 and disappearing permafrost.

51 **1. Introduction**

52 Due to the highly continental environment in northern Central Asia, Mongolia is subjected to dry and
53 winter-cold climate conditions. The landscape and vegetation development is highly sensitive to
54 changes in temperature and/or precipitation (Dulamsuren et al., 2010a; Gunin et al., 1999). The
55 intensity and impact of climate parameters on vegetation strongly varies in space caused by different
56 factors like topography, latitude and air circulation. Corresponding to the change of climatic
57 conditions from cold semi-humid in the north to warm and arid in the south, a latitudinal zonation of
58 the vegetation occurs, which is modified by an altitudinal zonation in the mountains (Hilbig, 1995).
59 From north to south, these vegetation zones include taiga, forest-steppe, steppe, and the Gobi
60 desert. Taiga, subtaiga, and fragmented forests in the forest-steppe ecotone represent the southern
61 edge of the Eurosiberian boreal forest, whereas the steppes are part of the Mongolian-Chinese
62 steppe region. The distribution of the different vegetation zones, boreal forest types, and treelines is
63 mainly controlled by air temperature, evapotranspiration, and precipitation (Walter and Breckle,
64 1994). However, site-specific edaphic parameters, including soil temperature, soil moisture and
65 nutrient availability also play a role. Moisture conditions are a key limiting factor controlling the
66 distribution of deserts and steppes as well as for the lower boundary of mountain forests at the
67 transition to drylands. In contrast, thermal conditions control position of the upper treeline and the
68 alpine vegetation belt (Körner, 2012; Klinge et al., 2015; 2003; Paulsen and Körner, 2014). Both, the
69 upper and the lower treelines of Mongolia's boreal forests represent an obvious visual boundary
70 between vegetation zones of highly different ecological requirements, though their actual state can
71 be strongly influenced by human impact (Klinge et al., 2015).

72 The mean temperature of the growing season (MGST) is more relevant for describing the thermal
73 environment at the upper forest line than mean annual air temperature (MAAT), because winter
74 temperatures are of minor significance for tree growth (Jobbágy and Jackson, 2000; Körner, 2012).
75 To define temperature conditions at the upper treeline the warmest month isotherm of 10 °C is
76 commonly used (Walter and Breckle, 1994). For the northern Tien Shan Mountains Klinge et al.
77 (2015) indicated a minimum monthly mean temperature of 5° C during the growing season. Paulsen
78 and Körner (2014) defined the minimum MGST of 5.5 to 7.5 °C and the mean temperature of 6.4 °C
79 during a period of daily temperatures >0.9 °C in a minimum growing season of 94 days for the upper
80 treeline in a global context. A lower treeline occurs in the semi-arid region of Central Asia between
81 relatively humid mountain regions and arid basins. The forest distribution is generally limited by
82 annual precipitation, which has its minimum between 300 and 200 mm y⁻¹ (Dulamsuren et al., 2010a;
83 Holdridge, 1947; Miede et al., 2003; Walter and Breckle, 1994).

84 In the forest-steppe, the spatial distribution of vegetation is highly correlated with terrain
85 parameters (Hais et al., 2016; Klinge et al., 2015). Less solar radiation input causes lower
86 temperatures and reduces the evapotranspiration pressure on north-facing slopes, leading to higher
87 humidity, higher soil moisture, and more widespread permafrost. The higher water availability
88 supports the tree growth (Dashtseren et al., 2014). The dominant tree species in Mongolia's boreal
89 forests is Siberian larch (*Larix sibirica*). On south-facing slopes higher solar irradiation produces

90 hydrological conditions which are too dry for the establishment of forests and thus favor grassland
91 (Bayartaa et al., 2007).

92 With respect to global climate change, the question of potential shifts in growth conditions arises.
93 Vegetation indices like the most commonly applied NDVI (Normalized differentiated vegetation
94 index) which are derived from multispectral satellite images (Landsat, MODIS, Spot VGT), provide
95 information about the “greenness” and vitality of the vegetation cover. The various investigations on
96 recent trends of climate and NDVI which exist for the region of Mongolia state partially diverging
97 results (Dashkhuu et al., 2015; Eckert et al., 2015; Miao et al., 2015; Poulter et al., 2013; Vandandorj
98 et al., 2015). Instrumental climate data from weather stations in Mongolia are often discontinuous
99 and time series of climate measurements are not available from mountain areas since climate
100 stations are located near settlements in the basins. Thus, representative climate parameters must be
101 modelled by different regionalization processes (Böhner, 2006). Various gridded datasets of re-
102 analyzed climate parameters with different spatial and temporal resolution exist, which are mainly
103 used for climate trend analysis; examples include CRU-TS (Harris et al., 2014), ERA-interim (Dee et al.,
104 2011), and CHELSA (Karger et al., 2017)(Figures S1 and S2 in the supplement material). While the
105 quality, origin, and resolution of climate records are potential sources of uncertainty, the results and
106 interpretations about the correlations between climate and NDVI trends occasionally suffer from
107 disregarding the specific bio-ecological restrictions of the different vegetation zones.

108 Batima et al. (2005) analyzed climate station data and observed an increasing MAAT of 1.7 °C for
109 Mongolia between 1940 and 2001. Eckert et al. (2015) stated that temperatures have not varied
110 much since the year 2000. Dulamsuren et al. (2014) found a trend to warmer temperature extremes
111 starting around 2000. Measurements of permafrost distribution and active layer development in
112 Mongolia show a general trend of permafrost degradation, which is accelerating since the 1990s
113 (Sharkhuu et al., 2007; Sharkhuu, 2003). This is due to climate warming, but reinforced by a loss of
114 vegetation caused by livestock grazing in some steppe areas and tree cutting in the forests.
115 Permafrost degradation is more intense in the Khuvsgul area than in the Khentei and Khangai
116 Mountains (Sharkhuu et al., 2007).

117 The trends of precipitation in Mongolia are not spatially uniform and can strongly depend on the
118 period of observation used for climate analysis (Erasmí et al., 2014; Giese et al., 2007). Batima et al.,
119 (2005) found a negative trend of annual precipitation in the period between 1970 and 2001. In the
120 driest regions of western and southern Mongolia no specific trends occurred at all. Based on tree-
121 ring data, Dulamsuren et al. (2010b) documented increasing drought stress for larch trees in the
122 Khentei Mountains, which they attributed to increasing aridity by rising summer temperatures and
123 decreasing summer precipitation during the last 50 years. Although trees at the outer boundary of
124 the forest stands might be better adapted to drought stress, obvious margins of dead trees
125 surrounding the forest islands are recently found at many places of the forest-steppe. For the period
126 from 1980 until 2005, Bayartaa et al. (2007b) reported a strong increase in burnt forest area in
127 Mongolia starting in 1996, which was caused by very dry winter and spring seasons but may also be
128 combined to weakened governmental management during the period of political transition. A
129 general tendency of decreasing lake levels during the last decades in two great lakes of interior
130 drainage in the Gobi with a catchment area south of Khangai Mountains was observed by
131 Szumińska (2016). This lake level decline was associated with trends for reduced precipitation and
132 increased evapotranspiration resulting from rising temperatures.

133 Eckert et al. (2015) analyzed the general trend for NDVI in Mongolia during the period between 2001
134 and 2011 using the MODIS NDVI dataset and found mostly positive trends in northern and eastern
135 Mongolia, stable conditions in southern Mongolia, and large areas of negative trends in the northern

136 Mongolian Altai and in the east of the Khangai Mountains. Based on the same dataset and a similar
137 period from 2000 to 2012, Vandandorj et al. (2015) analyzed the seasonal variation of NDVI for
138 individual vegetation zones. High variations of NDVI occur particularly in the steppe regions where
139 the vitality and density of grassland is closely related to the amount of annual precipitation due to
140 low stomatal control of transpiration by the grassland vegetation. Low variations in NDVI occur in
141 forested regions, since trees exert a much stricter stomatal control of transpiration than herbs and
142 grasses, and in the sparsely vegetated desert regions. Poulter et al. (2013) investigated the influence
143 of recent climate trends on the forests in Inner Asia by the temporal distribution of a greening value
144 using specific vegetation indices from remote sensing data and environmental datasets. They found a
145 trend to earlier greening induced by increasing spring temperatures and earlier browning associated
146 with decreasing summer precipitation. Based on these relationships they projected better future
147 forest conditions for Mongolia until 2100. In opposite of these findings, Bayartaa et al. (2007b)
148 reported that climate scenarios would indicate a significant decrease in forest area and its total
149 biomass for Mongolia until the middle of the 21st Century, which is in accordance with the recent
150 trends from dendrochronological data from Mongolia (Dulamsuren et al., 2010a; 2010b; 2014;
151 Khansaritoreh et al., 2017). Lu et al. (2014) investigated the applicability of different remote sensing-
152 based biomass estimation approaches. They found that the biomass estimation method via NDVI is
153 sufficient in low-density forests. Dulamsuren et al. (2016) showed the NDVI to be well usable to
154 estimate the tree biomass of Mongolian forests. The best fit of linear regression was found between
155 biomass and the mean NDVI of April for the period 1999-2013. This shows that in addition to the
156 vegetation vitality the NDVI is a valuable indicator for tree biomass in open forest stands.

157 With regard to the diverse and in parts contradicting observations on climate and vegetation status,
158 interdependencies, and recent trends in Mongolia that are reported here, this study investigates the
159 present distribution of forest areas and its relation to the actual climate and topography based on
160 high resolution satellite and gridded climate data. In addition to existing studies, here, the specific
161 impact of climate parameters related to different boreal forest types and ecological subunits is
162 analyzed in order to delineate potential turning points for environmental changes. The following
163 hypotheses were tested:

- 164 • Every type of boreal forest is delimited by a specific climatic envelope. The statistical correlations
165 between NDVI and climate parameters in different forest types and at the corresponding
166 treelines reflect climate-ecological relationships and limitations.
- 167 • Different spatial gradients of climate-induced vitality change exist for different types of boreal
168 forest. This applies in particular to the treelines as an indicator of extreme ecological site
169 conditions.
- 170 • Forest and grassland of the same zone of boreal forest type show different spatial gradients and
171 relations to climate.

172 2. The Study Area

173 Mongolia is situated in northern Central Asia in the transition zone between the Siberian taiga in the
174 north and the Gobi desert in the south (Fig. 1). Mongolia extends from 87°45'E to 119°56'E and from
175 41°34'N to 52°09'N and covers a total area of 1,562,950 km². Wide basins of interior drainage occur
176 at elevations between 900 and 1500 m a.s.l. with the lowest areas below 720 m a.s.l. There are five
177 principal mountain systems in Mongolia: The Mongolian Altai (MA) in the west (highest peak is Tavan
178 Bogd, 4374 m a.s.l.), the Gobi Altai in the south (Ikh Bogd, 3957 m a.s.l.), the Khangai Mountains
179 (KaM) in the center (Otgon Tenger, 3964 m a.s.l.), the Khentei Mountains (KeM) in the northeast
180 (Asralt Kharj khan, 2799 m a.s.l.), and the Khuvsgul region in the eastern Sayan Mountains (Munkh
181 Saridag, 3460 m a.s.l.). The mountain tops are shaped by pronounced flat surfaces at elevations
182 between 2500 and 3500 m a.s.l. (Academy of Sciences of Mongolia and Academy of Sciences of USSR,
183 1990; Murzaev, 1954)

184 The climate of Mongolia is highly continental with semi-humid, semiarid, and arid conditions. In
185 wintertime, the Siberian high pressure cell produces cold and dry weather with little snowfall and
186 mean temperatures between -15 and -30 °C (Barthel, 1983; Klinge, 2001). The main rainfall occurs
187 from June to August during the short summer and is induced by westerlies and cyclone precipitation,
188 with the dry season starting again in autumn. The mean summer temperatures range between 10
189 and 27 °C. Mean annual precipitation is lower than 50 mm in the interior basins, around 125 mm in
190 the southern desert and up to 350 mm in the northern steppes, whereas it rises to more than 500
191 mm in the high mountains.

192 According to the climatic conditions, the vegetation zones are arranged in characteristic sequences
193 along latitudinal and altitudinal gradients (Hilbig, 1995). Dark mountain taiga with coniferous trees
194 (*Pinus sibirica*, *Picea obovata*, *Abies sibirica*, *Larix sibirica*) occurs as closed forests in northern
195 Mongolia and locally as mountain taiga in the upper KaM in central Mongolia (Dulamsuren, 2004).
196 The subtaiga forest type with needle and deciduous broadleaf forests (*Larix sibirica*, *Pinus sylvestris*,
197 *Betula platyphylla*) represents a type of light taiga beneath and surrounding the mountain taiga. In
198 northern Mongolia, the forest often extends into the valley bottoms and open grassland is restricted
199 to intra-montane basins. The vegetation in central Mongolia consists of steppe grassland in the
200 basins and forest-steppe in the mountains. In this forest boundary ecotone of semiarid climate
201 conditions deciduous conifer forests consisting of *Larix sibirica* are primarily limited to north-facing
202 slopes (Treter, 1996). In the high mountains, dense alpine meadow vegetation occurs between
203 forest-steppe and the periglacial zone of frost debris. The main perennial rivers are accompanied by
204 floodplain meadows and alluvial forests of *Populus* and *Ulmus pumilla* (Hilbig, 1995).

205 Missing forest management and extensive forest use by tree cutting and wood pasture led to forest
206 degradation and local deforestation in many regions of Mongolia during the last decades
207 (Tsogtbaatar, 2004). In addition, hazardous forest fires destroyed large forest areas (Bayartaa et al.,
208 2007b; Goldammer, 2002; 2007; Hansen et al., 2013). Although it is supposed that most of the recent
209 forest fires in Mongolia were primarily set by humans, there is an additional ecological exposure to
210 fire susceptibility (Dorjsuren, 2009), which derived from climate warming, permafrost retreat, and
211 insect calamities.

212 3. Methods

213 Figure 2 shows a scheme of the complete analysis process and the individual steps are described in
214 detail below. Figure 3 provides visualizations of the different spatial resolution of the basic data sets
215 used for the analysis. The forested area of Mongolia and its surroundings was mapped from 50
216 Landsat 8 satellite images (spatial resolution 30 m). Images of the years 2013 and 2014 were used as
217 a baseline, and, in areas of low quality or high cloud coverage, were supplemented by Landsat 5
218 images from 2009 to 2011 (spatial resolution 30 m). The mapping process consists of two steps.
219 Initially a maximum likelihood supervised classification was carried out and subsequently the
220 resulting forest polygons were visually proofed and manually corrected.

221 The elevation of the actual treeline was calculated from selected points of a digital elevation model
222 (DEM) taken from SRTM-data (spatial resolution 90 m; Fig. 3c). Points representing the treeline were
223 established using a kernel-model, which evaluates for every pixel covered by forest if (1) it has a
224 slope of more than 2°, (2) there is any forested area in the surroundings in a higher or lower position,
225 and (3) there is any woodless area representing the existence of the next vegetation zone beyond the
226 potential forest boundary to exclude relief related distribution limits. The specific search parameters
227 for the upper and lower treeline are given in figure 2. Körner (2012) proposes a minimum vertical
228 range of 100 m from the upper treeline (UT) to the summit to prevent the summit effect on tree
229 development and to receive a true climatic treeline value. Due to extensive planation surfaces in the
230 area of KaM, the widespread alpine belt occurs with less than 100 m vertical distance between the
231 upper treeline and the flat mountaintops. Thus, it was necessary to reduce the minimum distance for
232 defining the summit effect in the modelling to only 10 m to prevent UT values beyond large alpine
233 areas from being excluded. After visual proof and deletion of strong outlying points, a final number
234 of 7,081 points for the UT and 5,220 for the lower treeline (LT) were used for the spatial
235 interpolation of the treeline surfaces applying the natural neighbor method (Watson, 1992).
236 Subsequently, the vertical distance of the treeline surfaces, the area above and below the treeline
237 were calculated. A buffer of 1000 m around these areas was chosen to represent the treeline
238 boundary area. This distance meets the spatial resolution of the Spot VGT and climate data (Fig. 3b).

239 The distribution of the different zones of boreal forest type was adapted from the Ecosystems Atlas
240 of Mongolia (Gunin and Vostokova, 2005). At places, where the map does not match the position of
241 the landscape elements represented in the remote sensing data, the spatial deviations were
242 corrected to the positions of the latter. The different ecosystem units were generalized to main
243 vegetation zones (desert, desert steppe, steppe, forest-steppe, subtaiga, taiga, alpine vegetation).
244 Forests of floodplain areas, which are hydrologically favored by groundwater, were excluded from
245 this analysis. Where forest areas were found in steppe regions, those parts were changed into forest-
246 steppe. In the upper elevation belts where the strong disparity between north-facing slopes with
247 forest and south-facing slopes with steppe dissipates, the areas with slopes covered by forests in
248 every direction were reclassified as mountain subtaiga. Subsequently, the mapped forest areas were
249 combined with the vegetation zones to achieve a spatial differentiation between forested area and
250 open grassland within the total ecological units (TE) of the forest-steppe, subtaiga and taiga. These
251 three types of boreal forest comprise the area under investigation in the present study.

252 Here, the statistical approach to use one mean value in a period of 15 years (1999-2013) for every
253 parameter was chosen in order to eliminate annual changes and inter-annual variations, which derive
254 from phenology and climate variability. Thus, normalized variables representing the mean site
255 conditions were computed and spatially analyzed, although this is a simplification since the plant
256 species respond to inter-annual variations and extreme values. NDVI, temperature and solar
257 radiation are integrated to the MGS. Precipitation during the winter season is retained in the soil and

258 additionally available during the MGS. The vegetation index from SPOT VGT satellite data was used
259 for the time span from January 1st, 1999 to December 31st, 2013, which originally consists of SPOT-
260 Vegetation 10-daily NDVI composites (spatial resolution 1 km, Fig. 3a). These data were aggregated
261 to monthly values using the maximum value of the three 10 day composites. Monthly NDVI data
262 were further aggregated to the mean of the growing season from May to September (MGS-NDVI) for
263 the period 1999 to 2013. We used re-analyzed climate data from the CHELSA dataset with 30 arc sec
264 resolution (approx. 1 km, Fig. 3b), because it incorporates terrain parameters and wind effect for
265 better representing climate parameters in the relief (Karger et al., 2016; 2017) (Figures S1 and S2 in
266 the supplement material). Monthly data from 1999 to 2013 were averaged to cover the same period
267 as the MGS-NDVI dataset. While mean growing season temperatures (MGST) were calculated from
268 the monthly means from May to September, the mean annual precipitation (MAP) represents the
269 average of the total annual sum of the period from 1999 to 2013. The sum of solar radiation input
270 (MGSR; Wh m⁻²) for the MGS (day 121-273) was simply calculated with a GIS-tool based on STRM-
271 DEM data for 2007 and was assumed to be relatively constant for the observation period 1999 to
272 2013.

273 Up to 3000 random points for both, forest and grassland area in the three types of boreal forest and
274 at the upper and lower forest boundary were chosen for statistical analysis (Tables 1, 2). The total
275 number of random points was reduced for treeline subunits, which have only a small spatial
276 distribution to prevent a too large point density. Areas of larger valleys where extensive forest occur
277 below the LT are excluded from the treeline analysis.

278 For each of the three boreal forest types (forest-steppe, subtaiga, taiga), first, the total area (total
279 ecological unit, TE) is considered, then, the TE is divided into forest (f) and grassland (s) and further
280 separated into the 1 km boundary area of both treelines (LT, UT). This categorization leads to 18
281 ecological subunits. Multiple comparisons between means were calculated with Duncan's multiple
282 range test after testing for normal distribution using SAS 9.4 software (SAS Institute Inc., Cary, North
283 Carolina, U.S.A.). In addition to the mean values, the standard deviation specifies the variation range
284 of the climate parameters for every subunit. Pearson and multiple correlation coefficients between
285 NDVI, MAP, MGST, and MGSR were computed as statistical base for the interpretation of regression
286 gradients. Due to the high amount of random points, it was opposed to perform a t-test because the
287 significance level (p-value) is always <0.05. The correlations at the level of the TE are used to analyze
288 the controlling climatic conditions and the environmental range with respect to the ecological
289 distribution of the entire type of boreal forest.

290 **4. Results**

291 **4.1 Treeline distribution**

292 The actual total area of Mongolian southern boreal forest was estimated at 73,818
293 km²(Dulamsuren et al., 2013). The proportion of forested areas related to the total areas of the ecological
294 units and subunits at the treelines are given in Table 3. The approximate forest proportion for all
295 three ecological units is 40 % and the highest proportions occur in the taiga and at all UT. As
296 expected for an ecotone low forest densities occur in the forest-steppe, but this is also true for LT of
297 all forest types. Figure 4 shows the forest distribution, the treelines, the vertical distance of the
298 forest belt, and the area beyond the treelines in northern Mongolia. No treeline continuance is
299 indicated in the southern part of Mongolia due to missing boreal forests in the desert. The treeline
300 distribution in western Mongolia generally corresponds to the results from (Klinge et al., 2003), who
301 investigated forest distribution in the Altai Mountains based on topographic maps.

302 Large areas above the UT occur in the MA, in the southern part of KaM and east of Lake Khuvsgul. In
303 the KeM areas above the treeline in >2500 m a.s.l. are small. The UTs show a general rise from 2200
304 m a.s.l. at the Mountains in the North ofUvs Nur and from 1800 m a.s.l. south of Lake Baikal to 2700
305 m a.s.l. in the southern parts of the MA and the KaM (Fig. 4a). At the southwestern side of the MA
306 the UT rises steeply from 2100 to 2600 m a.s.l. in a northeastern direction. In the large mountain
307 systems of the MA and KaM the UT stays in a relative constant altitude between 2400 and 2600 m
308 a.s.l. Northeast of KaM, the UT has an explicit longitudinal direction and a UT depression of up to 800
309 m occurs in the basin of the Selenga River. It was verified using the forest cover change data of
310 Hansen et al. (2013) that the extraordinary low UT in 1800 m a.s.l. is not related to burnt forest. At
311 large burnt areas, as they occur for example in the northern KaM, it could be expected that the
312 actual treeline is shifted and may not represent the natural limit. However, small forest patches
313 which remain vital still represent the potential forested area. Relic forest stands provide valuable
314 treeline values in the modelling process and help to identify areas of human or natural forest
315 disturbance (Klinge et al., 2015; Miede et al., 2003)

316 Large areas below the LT exist in the great basins and along the main river valleys, but they are also
317 present in the inter-montane basins (Fig. 4b). While the subtaiga is bordering to the meadow-steppe,
318 the lower treeline seldom occurs in the taiga and forests extend continuously into the valley bottom.
319 Nevertheless, at smaller inter-montane basins and valleys a lower forest boundary is still detectable
320 in the Mongolian taiga. Concordant with the intensifying aridity the LT is generally rising southward
321 from 1000 to 2500 m a.s.l. in eastern Mongolia. The strong rise of the LT at the north- and
322 southwestern slopes of the Altai Mountains is due to the convective rainfall at the western ranges
323 and the eastward intensification of aridity in the MA.

324 The forested area of central Mongolia, which remains between the large areas beyond the treelines,
325 is small from top-down view. However, the spatial expansion of forests has a particular vertical
326 component (Fig. 4c). The maximum altitudinal expansion of the forest belt of up to 1000 m vertical
327 distance occurs in the northwestern subtaiga and taiga. In the mountain forest-steppe of the central
328 MA, the western KaM, and in the mountains at Lake Khuvsgul, the altitudinal extent of forests
329 reduces below 400 m. In the southeastern part of the MA, the UT and LT converge, the forest belt
330 disappears, and the mountain steppe directly passes over into the alpine belt. Due to the
331 extraordinary low UT, thin forest belts also occur in the area northeast of the KaM and in the
332 southwestern part of KeM. This can be related to human impact by forest clearing in a more
333 populated region.

334 Most of precipitation is combined to westerlies, which produce humid condition at the western side
335 of the Altai Mountains. In the rain shadow at the eastern side in the central MA and in the Valley of
336 the Great Lakes dry conditions occur. This causes an extraordinary high LT and the small vertical
337 extent of the forest belt in this region (Klinge et al., 2003). The southern side of the KaM is still arid,
338 but its northern part and particularly the KeM receive more precipitation coming from the northeast
339 along the Selenga river depression. The tree species composition of the different boreal forest types
340 and subunits is given in Figure S3 in the supplement material.

341 **4.2 Specific climate parameters of boreal forest types**

342 The zonal statistics for the climate parameters and MGS-NDVI in different boreal forest types are
343 given in Table 1 and the correlation matrix between MGS-NDVI, MAP, MGST, and MGSR is presented
344 in Table 2. Fig. 5 illustrates the frequency distributions and linear regressions between these
345 parameters. The average MAP of the TE forests generally rises from 266 mm y⁻¹ in the forest-steppe
346 to 339 mm y⁻¹ in the subtaiga and 357 mm y⁻¹ in the taiga (Table 1). Due to the expected hydrological
347 limitation, the MAP at the LT is lower than the respective average of the TE. This is also true for all

348 forest subunits at the UTs, where the MAP is about 30 mm y⁻¹ lower than the mean average of the TE
349 forests. This phenomenon is due to the lower temperatures in higher mountains, which reduce the
350 evapotranspiration pressure. Moreover, the average MAP at the UT of the forest-steppe is even
351 lower than at the LT. However, sites with extremely low MAP below 190 mm y⁻¹ (Fig. 5a) receive
352 additional soil water supply. The grassland has predominantly lower average values of MAP than the
353 forest of the corresponding ecological unit. This general relation inverts at the UTs of the subtaiga
354 and taiga, while there are nearly equal values at the LTs of the forest-steppe and taiga.

355 The average MGST of any TEs are very similar between 11.0 and 11.7 °C. However, the maximum of
356 16 °C in the taiga is lower than in the forest-steppe and subtaiga where it is up to 18 °C (Fig. 5b).
357 While all average values of MGST at the LTs equate to the TE values, the UTs show frequency maxima
358 of the MGST between 7.5 and 8.9 °C (Table 1). With the exception of the UT in the subtaiga and taiga,
359 in all subunits, the grassland has similar or slightly higher temperatures as the forest of the same
360 unit. The phenomenon of an inversion of the general relation at the UT of the subtaiga and taiga,
361 which occurs simultaneously to the MAP, is due to a change of grassland vegetation. Alpine shrub
362 and meadow vegetation are supported by the cold and more humid climate and replace the
363 mountain meadow steppe. The MGST of all TEs and LTs shows similar frequency distributions with
364 wide value ranges and slightly higher values at the LTs (Fig. 5b). However, the narrow and uniform
365 frequency distributions of all UTs indicate that the MGST is the main controlling parameter for forest
366 distribution at the UT with an absolute minimum value of 6 °C. A considerable portion of MGST at the
367 UTs occurs between 10 and 13 °C, which is marginal in the forest-steppe and subtaiga but becomes
368 more important in the taiga.

369 **4.3 Relationship between climate and NDVI in different types of boreal forest**

370 The average values of MGS-NDVI of Table 1 show only small variation between the TE and the
371 treeline subunits. The values rise from forest-steppe to taiga and are higher in the forested area
372 compared to the grassland of the same subunit. The inverse relation between forest and grassland of
373 the same subunit, which occur for MAP and MGST at the UT of subtaiga and taiga, do not exist for
374 the NDVI. The frequency distributions of MGS-NDVI for the subunits in the forest-steppe are nearly
375 similar but clearly separated in the other types of boreal forest (Fig. 5c). The UTs have the lowest and
376 the TEs have the highest NDVI values, which is generally due to less favorable ecological site
377 conditions at the forest boundaries. In Table 2 most of the TEs show good correlations between NDVI
378 and the climate parameters ($r = 0.44-0.71$), with an obvious exception of the MAP and the taiga.
379 Linear regressions of the terrain parameter MGSR are omitted in Fig. 5, because MGSR is only weakly
380 correlated to the NDVI in all subunits.

381 In accordance with the correlation coefficients given in Table 2 the linear regressions between MGS-
382 NDVI, MAP, and MGST (Fig. 5) illustrates the relationship between the environmental conditions and
383 the types of boreal forest and their respective treelines. The regression trends indicate a potential
384 susceptibility of the ecological unit to climate changes. There are mostly low correlations between
385 MGS-NDVI and MAP at most subunits. The only exceptions are the TE and the LT of the forest-steppe
386 and particular the LT in the forest subunit of the taiga. However, the gradients of linear regression
387 indicate potential relations between NDVI and MAP for all LTs and particularly for all subunits in the
388 forest-steppe (Fig. 5a). Both, the correlation values and the linear regressions between MGS-NDVI
389 and MGST (Fig. 5b) indicate strong dependencies for all subunits; the UT of the forest-steppe is an
390 exception from this rule, since only weak correlation was found. However, the steep gradient of the
391 linear regressions at all UTs accentuates the temperature as the main limiting parameter with
392 increasing influence towards the taiga. Presupposing that at least precipitation, temperature and
393 solar radiation input control the vitality of the vegetation and the treeline distribution but with

394 different intensities for every subunit, the multi-regression correlations between NDVI and MAP,
395 MGST, and MGSR are generally higher. However, the combination of the two climate parameters
396 MAP and MGST shows the best correlations with the NDVI, while the combination of all three
397 parameters only leads to a marginal improvement (Table 2).

398 The high positive correlations between MAP and MGST and the high negative correlation between
399 MGST and MGSR in the TE and at the LT of the forest-steppe indicate a specific environmental
400 interrelation and potential auto-correlation effects between these two climate parameters in the
401 semiarid climate zone. This is due to the fact that in the forest-steppe the increasing atmospheric
402 vapor pressure deficit, which results from higher temperatures, must be compensated by more
403 precipitation, on the one hand, and by less solar radiation input, on the other hand. However, the
404 weak correlation between MAP and MGST in all subunits of the subtaiga and taiga indicate a climate
405 independent factor. This is notably attributable to permafrost distribution as a supplemental
406 ecological parameter, which is not included in our regression models but modifies the soil
407 hydrological regime. Regression gradients between MAP and MGST of the TEs change from the
408 strong positive gradient in the forest-steppe into a less precipitation-dependent gradient in the
409 subtaiga and then into a negative gradient in the taiga (Fig. 5d). The rising MAP produces more
410 humid climate in the taiga and reduces the dependency of vegetation vitality in the TE on
411 precipitation limits. Low temperatures as zonal climatic parameter become a dominating limit for
412 tree development towards higher latitudes. Concordant to the transformation of ecological
413 conditions, the physiological constitution of individual trees and the tree species composition
414 changes from drought-adapted to low-temperature adapted but more drought sensitive individuals.

415 5. Discussion

416 Trees grow and exist for several decades or centuries and establish an autochthonous microclimate
417 below the canopy, thus forests are representing mean climatic conditions of a longer period. In
418 contrast, the vitality of annual or perennial grasses and herbs of the steppes and meadows respond
419 to inter-annual variation in climate conditions and the vegetation density represents small-scale
420 periods (Bat-Oyun et al., 2016). The treelines represent boundaries of forest distribution at the
421 ecological limits and it is hypothesized that changes in climate or environmental conditions at these
422 boundaries lead to an alteration of the treelines. On the one hand forest expansion needs a longer
423 period of favorable conditions for seed formation, as well as seedling and sapling establishments. The
424 requirements can be different from those of mature trees. On the other hand, declines in the forest
425 area can be induced by short hazardous events like drought, freeze, calamities, or fire. Human impact
426 on the forest area since prehistoric times is another important influence on the actual treeline
427 (Klinge et al., 2015; Miede et al., 2003). Treeline might be shifted as the result of changes in climate
428 changes with a certain time lag. Although the treeline may not directly correspond to the current
429 climatic envelope for forest, it represents at least the minimum of potential forest area. In view of
430 the ecological relations, the spatial accuracy of the actual database, and the regional scale of the
431 investigation, it is reasonable to calculate average values for a longer period to receive
432 representative parameters.

433 The lower boundaries of the distribution curves (Fig. 5a) and the standard deviation of MAP (Table 1)
434 indicate that an approximate MAP of 190 mm y^{-1} can be regarded as the minimum amount of direct
435 rainfall for tree development in Mongolia. Dulamsuren et al. (2010a) reported an annual
436 precipitation between 230 and 400 mm for larch trees (*Larix sibirica*) at the lower forest boundary in
437 northern and central Mongolia. For the northern Tian Shan Mountains Klinge et al. (2015) state a
438 minimum MAP of 250 mm for the distribution limit of spruce trees (*Picea schrenkiana*). Sites with
439 lower MAP values, occurring in parts of the forest-steppe, are favored by additional soil water supply

440 from upslope area or melting permafrost ice, which can support tree growth under these dry
441 conditions where rainfall is insufficient (Dulamsuren et al., 2014). This explains why Dulamsuren et al.
442 (2014) found coniferous forests in regions with an annual precipitation of around 120 mm in the MA.
443 The annual amount of precipitation is highly varying in the steppes region and the permafrost layer
444 can bridge drought years by accumulating soil water in the soil ice reservoir during moist years
445 (Sugimoto et al., 2002). The vegetation vitality as expressed by the NDVI is generally lower in the
446 forest-steppe than in the subtaiga and the taiga. This fact reflects the extreme ecological limitations
447 of forests in the forest-steppe ecotone. Recently emerging margins of dead trees around the forest
448 islands are apparently induced by the trend of increasing temperature, insufficient precipitation, and
449 missing soil water storage from disappearing discontinuous permafrost.

450 The proportion between open grassland area and forest islands in the southern forest-steppe
451 changes towards northern latitudes with the expansion of forest area. In the large valleys of the taiga
452 and subtaiga in northern Mongolia, where trees are apparently less limited by water shortage, a LT
453 does not exist. However, inside the dense woodland of the taiga, the grassland occurs in intra-
454 montane basins (Dulamsuren et al., 2005; Gunin et al., 1999; Hilbig, 1995). The rain shadow of the
455 surrounding mountains keeps precipitation extraordinarily low and thus a LT is present. The high
456 correlation of the detected LTs to MAP in the taiga suggests a primarily drought-induced and not
457 anthropogenic position of the LT. This finding points to a high vulnerability of the trees at the taiga's
458 LT to climate warming. This conclusion is supported by ecophysiological, dendrochronological, and
459 palynological studies from the LT of the mountain taiga of western Khentei (Dulamsuren et al.,
460 2009a; 2010b; Schlütz et al., 2008).

461 There is a close correlation between NDVI and MGST at the UT in the taiga and the subtaiga (Table
462 2). At the UT of the forest-steppe, precipitation is an additional limiting factor at higher elevations.
463 While a MGST of 6 °C tends to be the general minimum temperature for tree growth in the study
464 area, at some places at the UT of the subtaiga, trees occur at MGST as low as 4 °C (Fig. 5b). Here, the
465 low MGST is associated with high MAP of roughly 350 mm y⁻¹ (Fig. 5d). In the low temperature range
466 between 6-8 °C, the linear regressions between MAP and MGST at the UT show that different MAP
467 conditions exist simultaneously for the different types of boreal forest (Fig. 5d). In the forest-steppe
468 at 6 °C MGST, MAP is approximately 200 mm y⁻¹, whereas it amounts to 320 mm y⁻¹ in the subtaiga
469 and 400 mm y⁻¹ in the taiga. This combination between both low precipitation and temperature is
470 extreme at the LT of the forest-steppe. In the range of 6-8 °C MGST, MAP tends to be below the tree
471 growth minimum of 190 mm y⁻¹, which emphasizes again the impact of permafrost, as the
472 permafrost is also associated with low temperatures.

473 Differing frequency distributions show that the NDVI at the UT and LT is generally lower than in the
474 TEs of the taiga and the subtaiga, except for the forest-steppe (Fig. 5c). The low NDVI values indicate
475 low vegetation vitality. This suggests that forests composing the treelines in the taiga and the
476 subtaiga and the complete forest-steppe ecotone are exposed to physiological stress. Forests in the
477 taiga receive generally more precipitation and thus have developed higher stand densities and are
478 also home to more water-demanding dark taiga tree species (Dulamsuren, 2004; 2010a). Reports of
479 increased drought stress, reduced stemwood formation, reduced forest regeneration and increased
480 tree mortality especially in the *Larix sibirica*-dominated forest-steppe ecotones of Inner Asia support
481 this conclusion (Dulamsuren et al., 2010a; 2010b; 2013; Liu et al., 2013).

482 Recent climate change scenarios predict a temperature increase in Mongolia of up to 5 °C until the
483 end of the century (Ministry of the Environment Japan, 2015), while projections for precipitation
484 trends show spatial differences between decreasing precipitation amounts in the north and increase
485 in the southern parts (Sato et al., 2007). In general, climate modelling also suggests an future

486 increase of summer droughts and a decrease of soil moisture (Sato et al., 2007). Higher temperatures
487 yield to higher evapotranspiration and hence to less relative humidity, even if a slight increase of
488 precipitation simultaneously occurs. The consequences of increasing aridity and an increasing
489 atmospheric vapor deficit are a reduction in tree vitality, which finally might lead to widely increased
490 tree mortality and forest area loss in the forest-steppe, subtaiga, and taiga. In addition, this trend
491 could promote of *Pinus sylvestris* in parts of the *Larix sibirica*-dominated forest-steppe (Dulamsuren
492 et al., 2009b).

493 **6. Conclusion**

494 Using high resolution remote sensing and climatic data allows characterizing the climatic envelope of
495 the three types of boreal forest in Mongolia and to identify hotspots of additional natural or
496 anthropogenic factors. It was shown that the NDVI distribution between forest and grassland of the
497 same ecological subunits differ, which is mainly controlled by different photosynthetic activity,
498 vegetation density, and seasonal growth. However, with respect to the small-scale variation of the
499 vegetation and the resolution of the NDVI-data a spatial overlap producing mixed data values cannot
500 be totally avoided. The ecological relationship between climatic parameters and forest or treeline
501 distribution was verified by the NDVI as an indicator for vegetation vitality. It can be assumed that
502 local site conditions like permafrost distribution, soil parameters and hydrology may also play an
503 important role for vegetation vitality. The statistical results on geo-ecological relations presented in
504 this work are suited to be used for modeling of potential past, actual, and future forest area.

505 The observed recent increase of forest greening indices from remote sensing data and stemwood
506 increment found in several places by Poulter et al. (2013) is combined to increasing summer
507 temperature but also promoted by additional soil water supply from melting permafrost. However,
508 disappearing permafrost and increasing drought stress, as projected by climate modelling, may cause
509 dramatic forests cover loss in future. The widespread occurrence of dead tree margins around forest
510 islands shows that this trend is already ongoing as the result of climate warming. Trees suffering from
511 drought stress are more vulnerable to insect calamities. The impact of forest fires also increases
512 under dryer conditions. For all LTs and for the TE of the forest-steppe, increasing temperatures are
513 likely to result in increased tree mortality, the reduction of forested area, and shifting of the LTs.

514 Research on NDVI trends and climate development in Mongolia is often lacking detailed spatial
515 separation of the different ecological units. Every vegetation unit has its own temporal defined
516 ecological environment, which produces different spatial and temporal gradients in remote sensing
517 derived vegetation indices. Changes in climate conditions will lead to more or less vitality in the
518 limited physiological range of the individual trees, which are adapted to recent local climate and soil
519 conditions. Forest dynamics and forest development from the biological point of view means change
520 in the vegetation structure and biodiversity, which cannot be exclusively modelled by greening
521 indices (Busing and Mailly, 2004; Miao et al., 2015; Poulter et al., 2013). It was shown, that the
522 creation of detailed landscape stratification and of small-scaled ecological classifications could assist
523 to incorporate spatial and temporal transitions of vegetation units in environmental modelling.

524 **Acknowledgements**

525 The authors would like to thank the US Geological Survey and VITO, Belgium for making the satellite
526 data freely available for scientific research. We acknowledge support by the Open Access Publication
527 Funds of Göttingen University. We very specially thank Dr. Jan Degener for his scientific support in
528 data processing and intensive discussion. We also thank Prof. Dr. Udo Schickhoff and an anonymous
529 referee for the valuable comments to improve the manuscript.

- 530 Funded by the Deutsche Forschungsgemeinschaft (DFG) – Projektnummern FR 877/32 and DU
531 1145/4-1
- 532 This open-access publication was funded by the University of Göttingen.

533 Tables:

534 Table 1: Arithmetic mean \pm standard deviation of different climate parameters (MAP: Mean Annual
 535 Precipitation, MGST: Mean Growing Season Temperature, MGS-NDVI: Mean Growing Season
 536 Normalized Differentiated Vegetation Index) and vegetation units (Subunits are TE: Total Ecological
 537 unit, LT: Lower Treeline, UT: Upper Treeline, s: portion of grassland, f: portion of forest). Within one
 538 row, mean values sharing a common uppercase letter, do not differ significantly ($P \leq 0.05$, Duncan's
 539 multiple range test, $df_{\text{model}} = 2$). Within one subunit (forest-steppe, subtaiga, taiga), mean values
 540 sharing a common lowercase letter, do not differ significantly ($P \leq 0.05$, Duncan's multiple range test,
 541 $df_{\text{model}} = 5, 13295$).

| Subunit | Forest-steppe | Subtaiga | Taiga |
|---------------------------|--------------------|--------------------|--------------------|
| MAP (mm y ⁻¹) | | | |
| TE _f | 266 \pm 62 Aa | 339 \pm 70 Ba | 357 \pm 69 Ca |
| TE _s | 256 \pm 63 Ab | 309 \pm 68 Bbe | 331 \pm 73 Cb |
| LT _f | 251 \pm 60 Ac | 294 \pm 60 Bc | 292 \pm 56 Bc |
| LT _s | 253 \pm 62 Abc | 286 \pm 57 Bd | 290 \pm 53 Bc |
| UT _f | 231 \pm 52 Ad | 305 \pm 72 Be | 333 \pm 80 Cbd |
| UT _s | 227 \pm 54 Ae | 314 \pm 73 Bb | 339 \pm 80 Cd |
| MGST (°C) | | | |
| TE _f | 11.0 \pm 2.1 Aa | 11.7 \pm 2.3 Ba | 11.1 \pm 1.4 Ca |
| TE _s | 11.6 \pm 2.5 Ab | 11.7 \pm 2.7 Ba | 11.1 \pm 1.7 Ca |
| LT _f | 11.5 \pm 2.2 Ab | 12.1 \pm 2.6 Bb | 11.5 \pm 1.7 Ab |
| LT _s | 12.1 \pm 2.3 Ac | 12.8 \pm 2.4 Bc | 11.7 \pm 1.6 Cc |
| UT _f | 8.4 \pm 0.8 Ad | 7.9 \pm 1.2 Bd | 8.9 \pm 1.3 Cd |
| UT _s | 8.4 \pm 0.9 Ad | 7.5 \pm 1.2 Be | 8.5 \pm 1.3 Ce |
| MGS-NDVI | | | |
| TE _f | 0.51 \pm 0.08 Aa | 0.60 \pm 0.08 Ba | 0.63 \pm 0.06 Ca |
| TE _s | 0.47 \pm 0.08 Ab | 0.55 \pm 0.09 Bb | 0.55 \pm 0.09 Cb |
| LT _f | 0.46 \pm 0.08 Ab | 0.54 \pm 0.08 Bc | 0.58 \pm 0.09 Cb |
| LT _s | 0.44 \pm 0.08 Ac | 0.51 \pm 0.08 Bd | 0.55 \pm 0.08 Cc |
| UT _f | 0.44 \pm 0.06 Ac | 0.47 \pm 0.07 Be | 0.51 \pm 0.09 Cd |
| UT _s | 0.42 \pm 0.07 Ad | 0.44 \pm 0.08 Bf | 0.47 \pm 0.09 Ce |

542

543

544 Table 2: Correlation matrix showing Pearson and multiple correlation coefficients (r) between NDVI,
 545 climate, and terrain parameters for different types of boreal forest and ecological subunits. (MAP:
 546 Mean Annual Precipitation, MGST: Mean Growing Season Temperature, MGS-NDVI: Mean Growing
 547 Season Normalized Differentiated Vegetation Index, MGSR: Mean Growing Season Solar Radiation
 548 Input, subunits are TE: Total Ecological unit, LT: Lower Treeline, UT: Upper Treeline, s: portion of
 549 grassland, f: portion of forest)

| Subunit | Forest-steppe | Subtaiga | Taiga | Forest-steppe | Subtaiga | Taiga | Forest-steppe | Subtaiga | Taiga | Forest- steppe | Subtaiga | Taiga |
|-----------------|-----------------------|----------|-------|----------------------|-------------|-------------|-----------------------|-------------|-------------|------------------------------|-------------|-------------|
| | MGS-NDVI / MAP | | | MGS-NDVI / MGST | | | MGS-NDVI / MGSR | | | | | |
| TE _f | 0.58 | 0.44 | 0.22 | 0.49 | 0.62 | 0.55 | -0.15 | -0.24 | -0.09 | | | |
| TE _s | 0.57 | 0.38 | 0.19 | 0.49 | 0.55 | 0.57 | -0.26 | -0.17 | -0.18 | | | |
| LT _f | 0.53 | 0.33 | 0.51 | 0.56 | 0.52 | 0.60 | -0.09 | -0.20 | -0.18 | | | |
| LT _s | 0.55 | 0.39 | 0.39 | 0.61 | 0.52 | 0.46 | -0.29 | -0.29 | -0.30 | | | |
| UT _f | 0.34 | 0.11 | 0.34 | 0.31 | 0.59 | 0.71 | 0.22 | 0.19 | 0.08 | | | |
| UT _s | 0.42 | 0.10 | 0.33 | 0.25 | 0.55 | 0.66 | 0.15 | 0.17 | 0.08 | | | |
| | MGS-NDVI / MAP ; MGSR | | | MGS-NDVI/MGST ; MGSR | | | MGS-NDVI / MAP ; MGST | | | MGS-NDVI / MAP ; MGST ; MGSR | | |
| TE _f | 0.58 | 0.47 | 0.24 | 0.51 | 0.62 | 0.56 | 0.62 | 0.71 | 0.64 | 0.63 | 0.72 | 0.65 |
| TE _s | 0.58 | 0.41 | 0.26 | 0.50 | 0.56 | 0.58 | 0.62 | 0.67 | 0.68 | 0.63 | 0.67 | 0.68 |
| LT _f | 0.53 | 0.36 | 0.52 | 0.59 | 0.52 | 0.60 | 0.60 | 0.56 | 0.72 | 0.63 | 0.57 | 0.72 |
| LT _s | 0.56 | 0.43 | 0.42 | 0.61 | 0.52 | 0.50 | 0.64 | 0.58 | 0.57 | 0.65 | 0.58 | 0.58 |
| UT _f | 0.36 | 0.24 | 0.35 | 0.37 | 0.60 | 0.71 | 0.43 | 0.62 | 0.74 | 0.45 | 0.64 | 0.75 |
| UT _s | 0.42 | 0.21 | 0.34 | 0.30 | 0.56 | 0.66 | 0.47 | 0.58 | 0.69 | 0.47 | 0.59 | 0.69 |
| | MAP / MGSR | | | MGST / MGSR | | | MAP / MGST | | | | | |
| TE _f | -0.23 | -0.16 | 0.05 | -0.54 | -0.48 | -0.29 | 0.50 | 0.16 | -0.18 | | | |
| TE _s | -0.29 | -0.05 | 0.01 | -0.67 | -0.42 | -0.26 | 0.47 | 0.00 | -0.28 | | | |
| LT _f | -0.22 | -0.21 | -0.16 | -0.46 | -0.47 | -0.24 | 0.63 | 0.23 | 0.20 | | | |
| LT _s | -0.37 | -0.29 | -0.41 | -0.58 | -0.44 | -0.23 | 0.65 | 0.24 | 0.12 | | | |
| UT _f | 0.25 | -0.18 | 0.01 | 0.05 | 0.11 | 0.04 | 0.12 | -0.11 | 0.18 | | | |
| UT _s | 0.20 | -0.10 | -0.05 | 0.00 | 0.12 | 0.16 | 0.11 | -0.15 | 0.17 | | | |

550

551

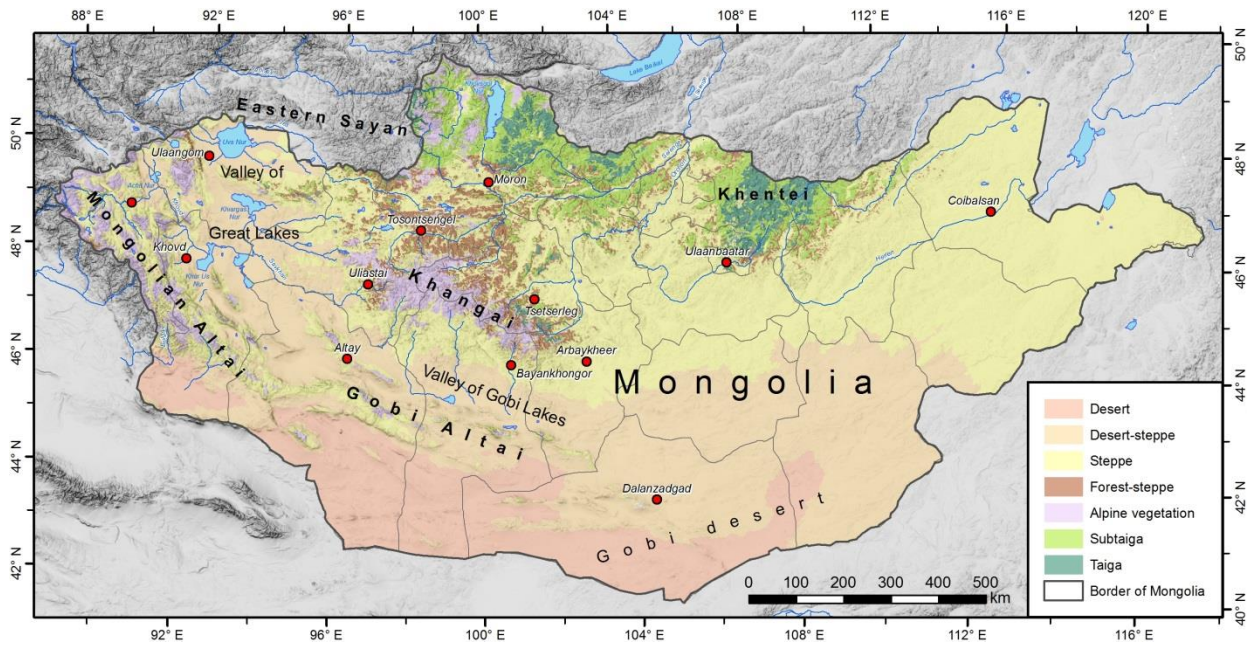
552 Table 3: Proportion of forest area (f) and total area of different boreal forest types and corresponding
 553 treelines. (TE: Total Ecological unit, LT: Lower Treeline, UT: Upper Treeline)

554

| area km ² | TE | TE _f | % _f | LT | LT _f | % _f | UT | UT _f | % _f |
|----------------------|---------|-----------------|----------------|--------|-----------------|----------------|-------|-----------------|----------------|
| Forest-steppe | 62,678 | 17,983 | 28.7 | 17,275 | 3,894 | 22.5 | 3,525 | 1,822 | 51.7 |
| Subtaiga | 87,648 | 38,747 | 44.2 | 7,558 | 2,135 | 28.2 | 3,168 | 1,341 | 42.3 |
| Taiga | 31,710 | 17,088 | 53.9 | 1,234 | 401 | 32.5 | 949 | 495 | 52.2 |
| Sum | 182,036 | 73,818 | 40.6 | 26,067 | 6,430 | 24.7 | 7,642 | 3,658 | 47.9 |

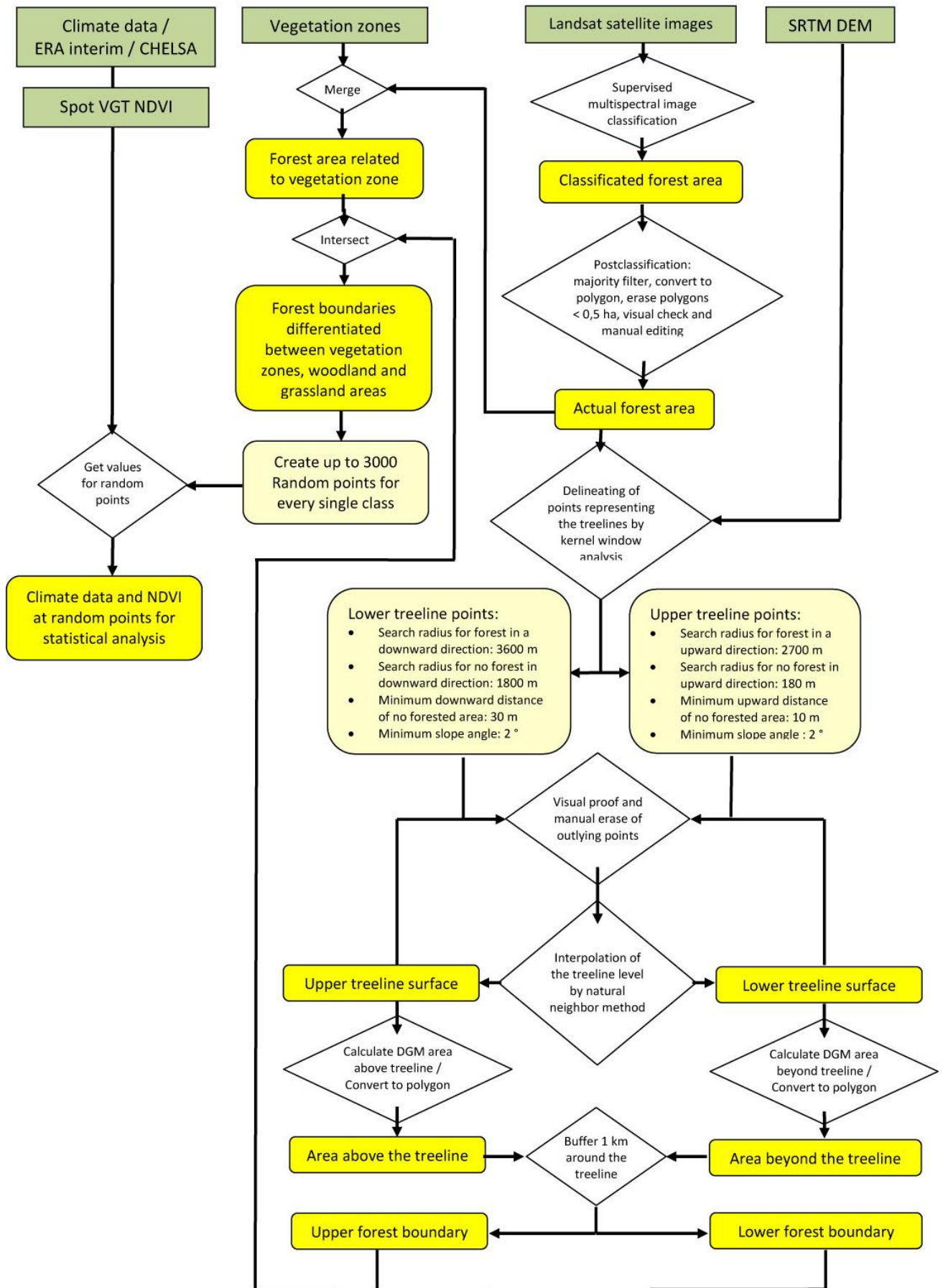
555

556 Figures:



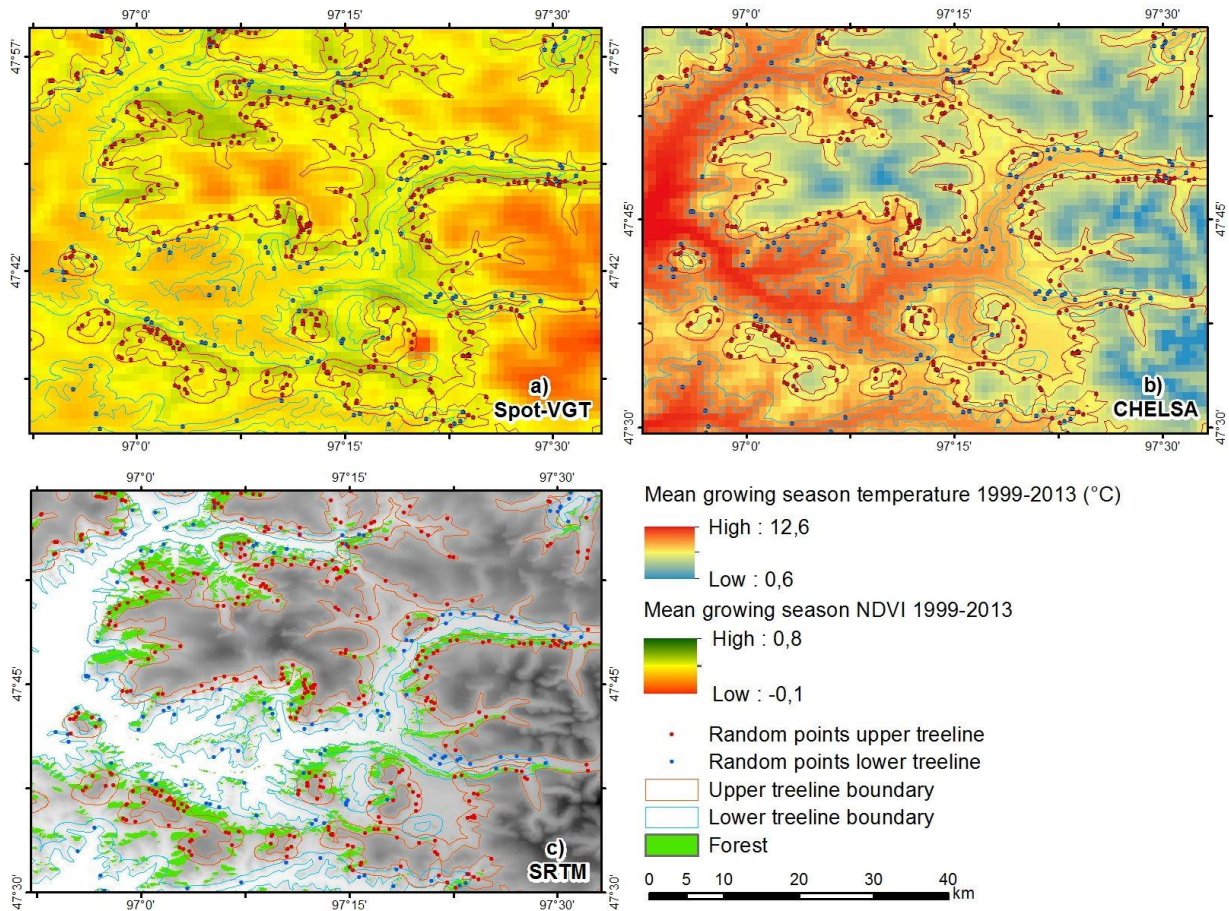
557

558 Figure 1: The vegetation zones of Mongolia (modified from Gunin and Vostokova, (2005) and Landsat
559 8 supervised classification).



560
561
562

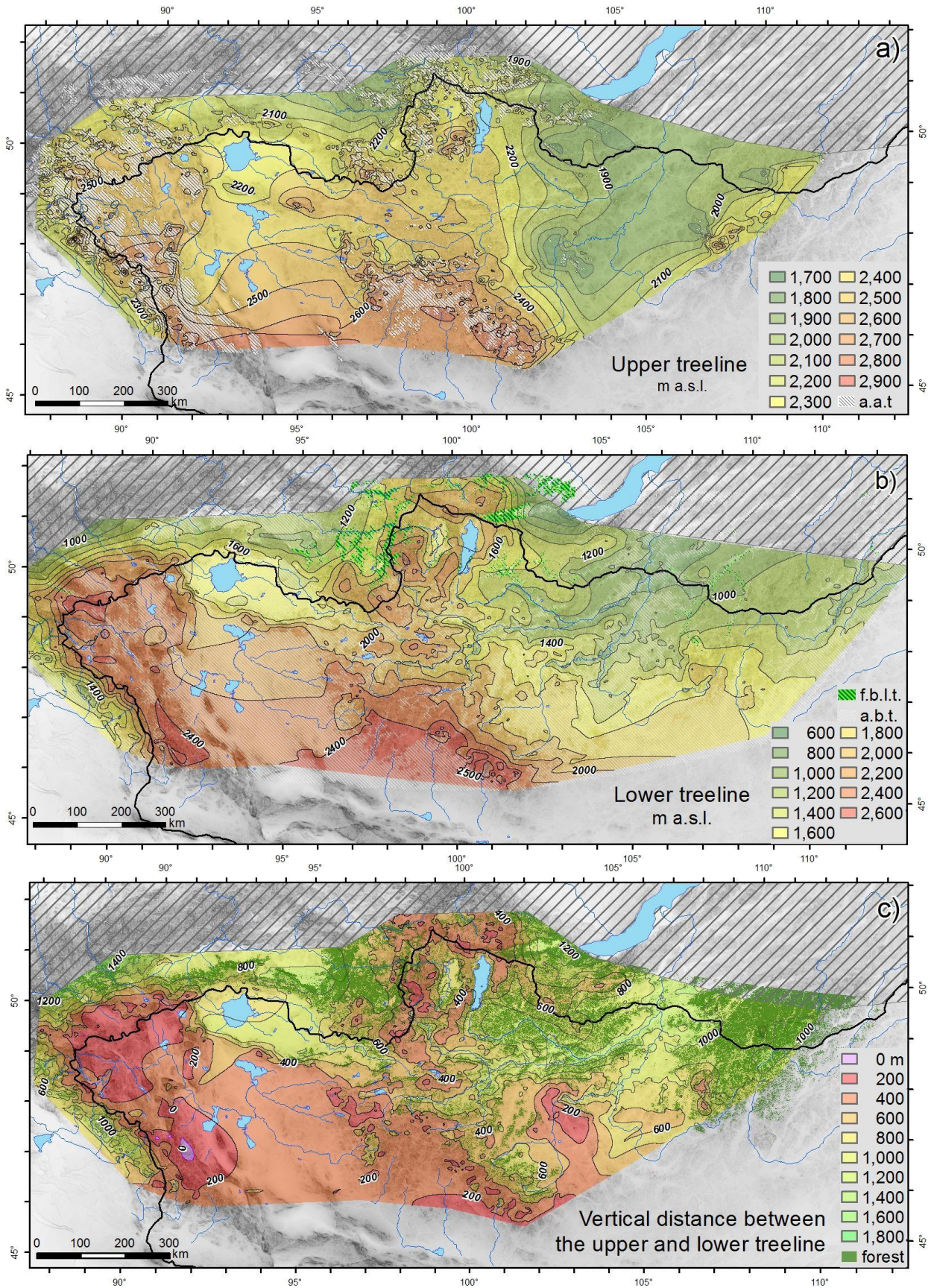
Figure 2: Processing workflow for treeline delineation, NDVI and climate analysis.



563

564 Figure 3: Examples for the spatial resolution of the different data: (a) mean growing season NDVI
 565 1999-2013, (b) mean growing season temperature 1999-2013, (c) upper and lower treeline boundary
 566 from Landsat and SRTM data.

567

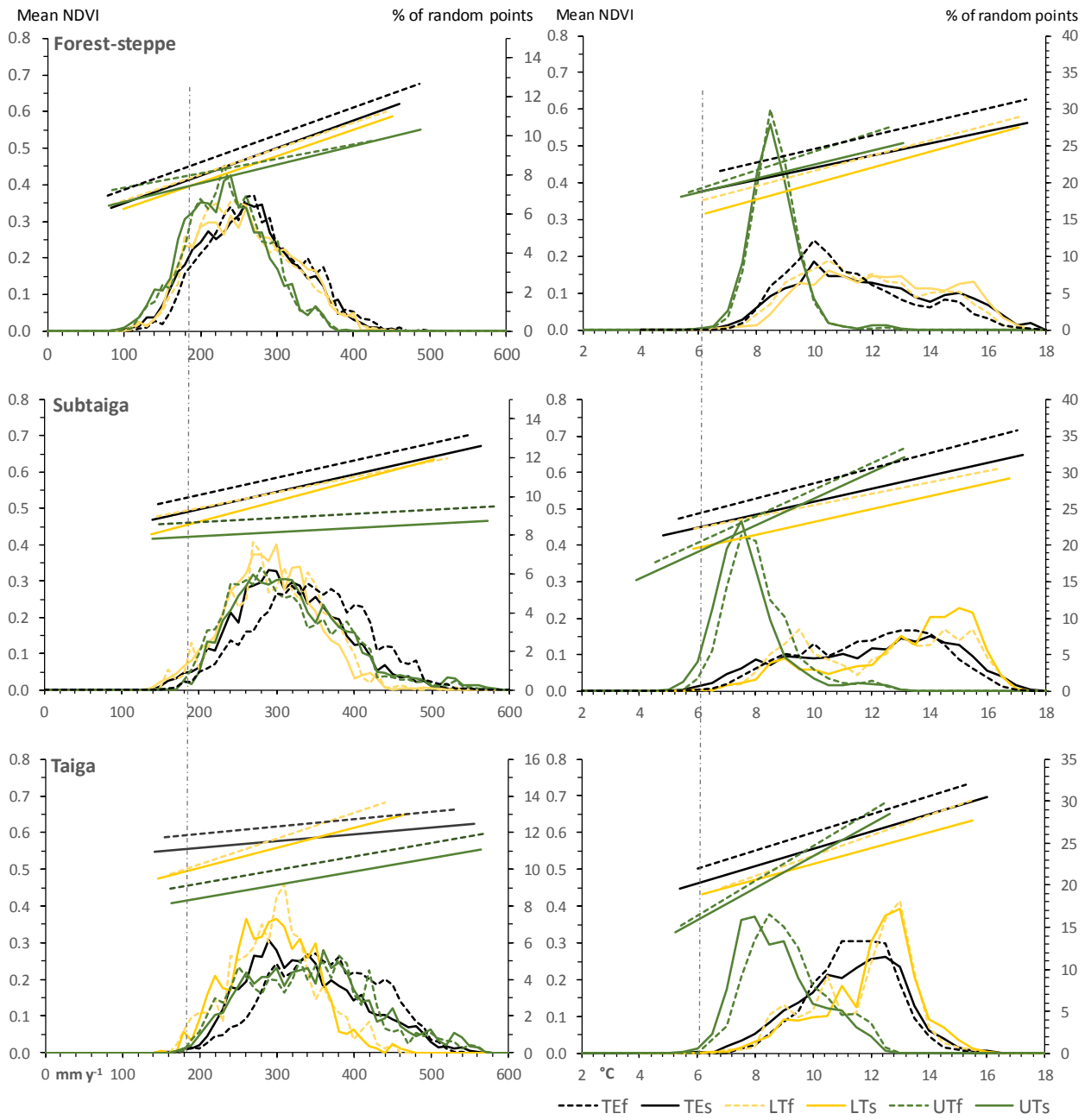


568

569 Figure 4: Treeline distribution maps of Mongolia: (a) upper treeline, (b) lower treeline, (c) vertical
 570 distance between upper and lower treeline (a.a.t. = area above the upper treeline, a.b.t. = area
 571 beneath the lower treeline, f.b.l.t. = forest below the lower treeline)

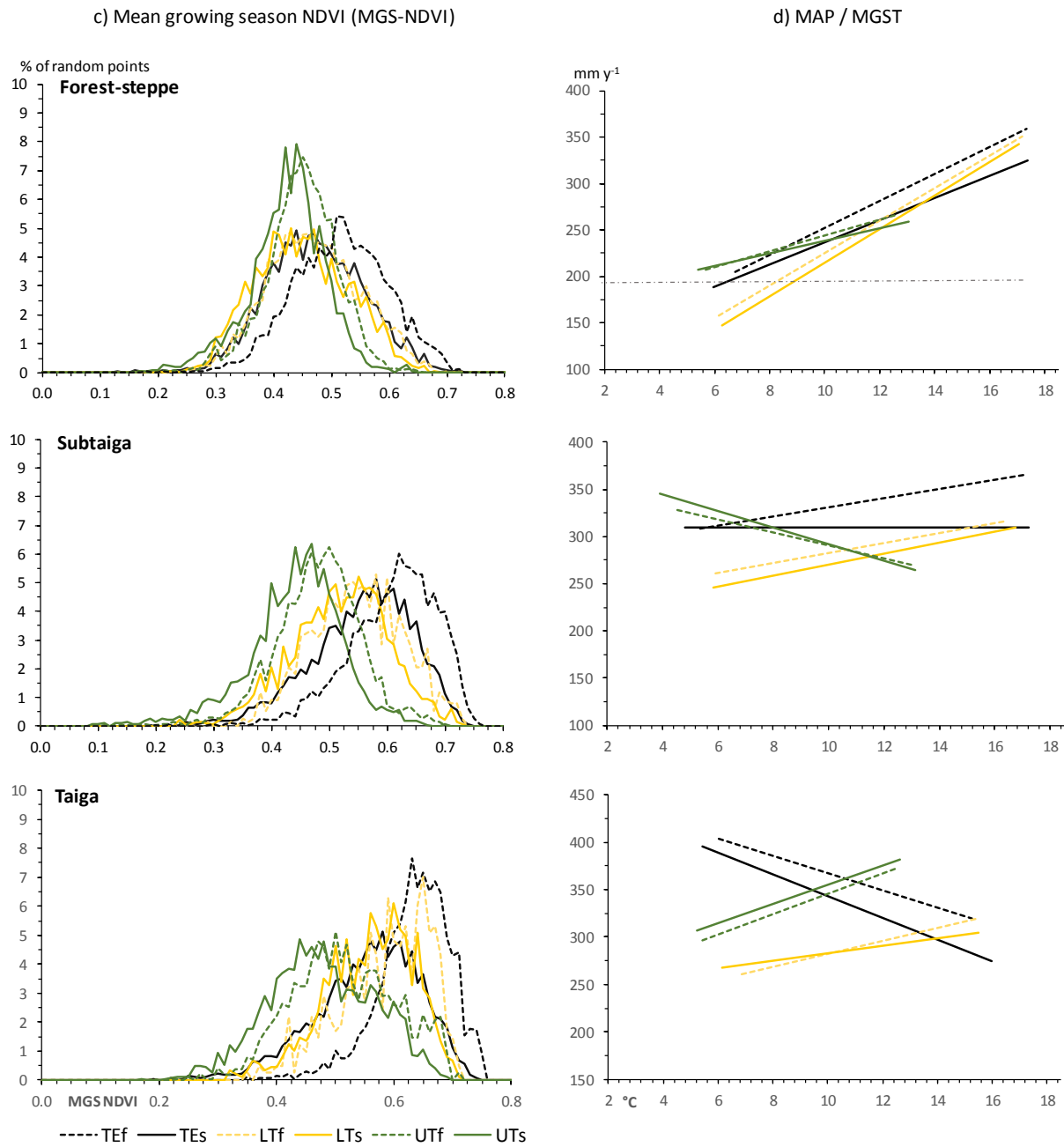
a) Mean annual precipitation (MAP)

b) Mean growing season temperature (MGST)



572
573

Figure 5 (continued)

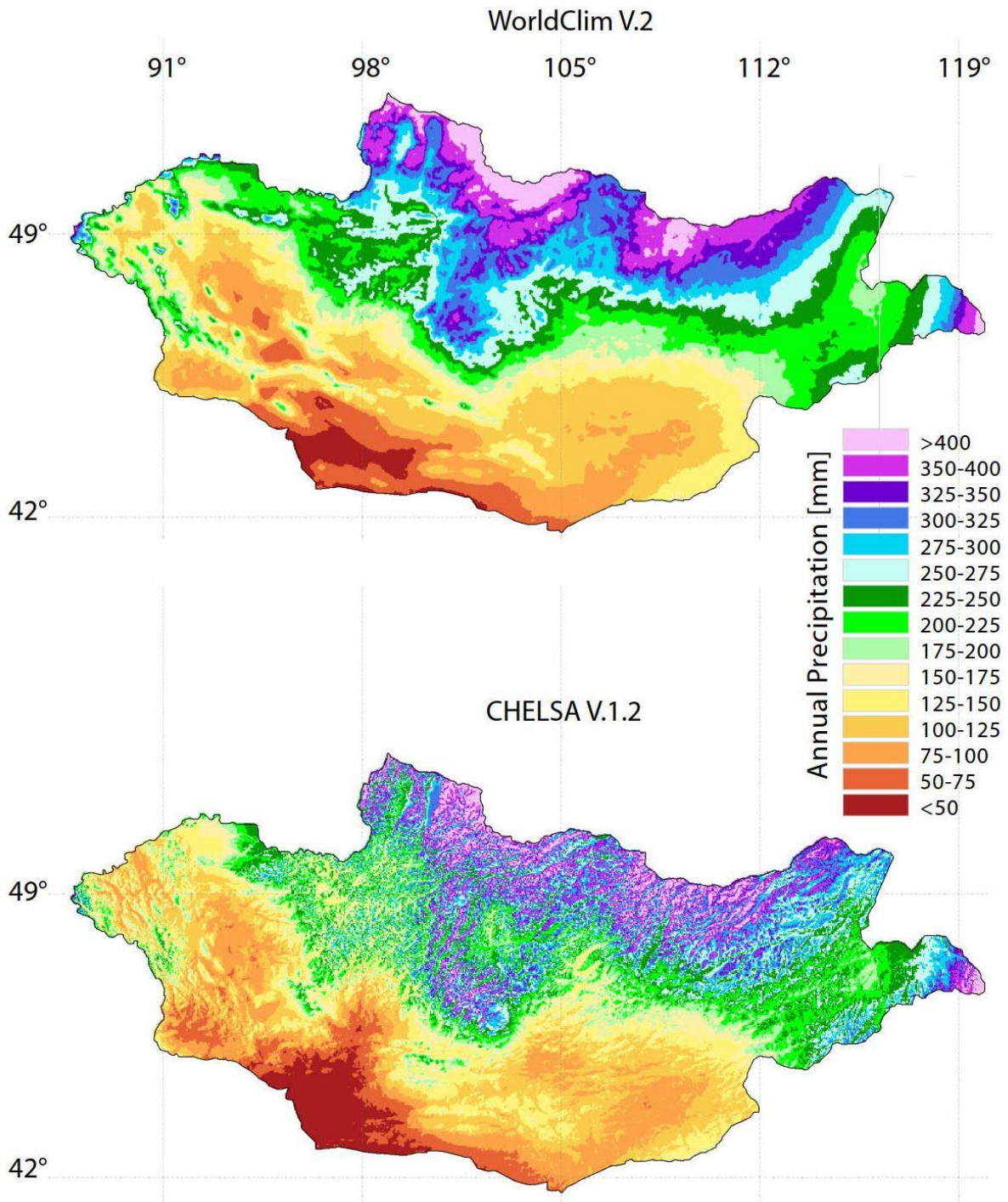


574

575 Figure 5: Mean annual precipitation (MAP) and mean air temperature during the growing season
 576 (MGST) related to the mean growing season NDVI of random points of different ecosystem units
 577 (values averaged for the investigation period 1999-2013). The straight lines are representing the
 578 linear regressions between climate parameters and NDVI. The distribution curves represent the
 579 frequency of random points (%). Dashed lines represent forest values (f); continuous lines represent
 580 grassland values (s); yellow colors represent lower treeline values (LT); green color represents upper
 581 treeline values (UT) and black colors represent the total ecological unit values (TE). Vertical grey
 582 dashed lines indicate the deduced minimum values for tree growth.

583

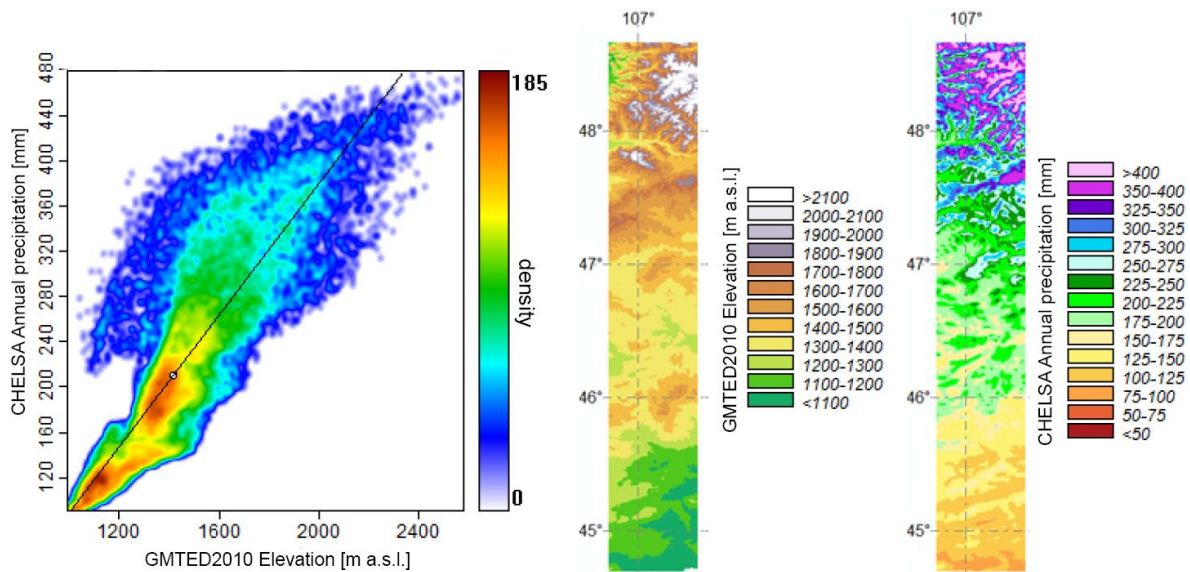
584 Supplement material:
585



586 **Figure S1:** Comparison of mean annual precipitation sums from two different datasets (CHELSA V1.2)
587 and (WorldClim V.2) for Mongolia. Both climatologies show similar patterns on the macro
588 geographical scale, but deviate on the micro scale. Note that these two datasets also differ in their
589 temporal extent (Worldclim: 1970-2000, CHELSA: 1979-2013).

590

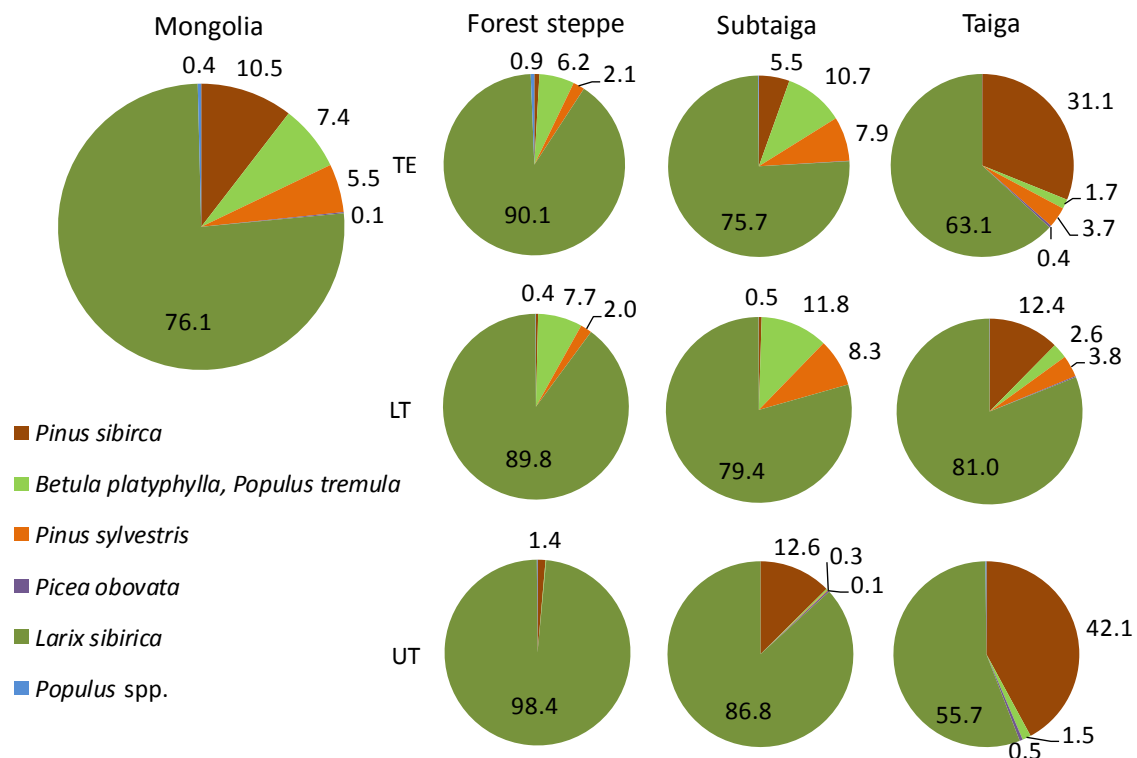
591



592 **Figure S2:** Annual precipitation along an elevational gradient in the region of Ulaanbaatar, Mongolia.
 593 To produce the scatterplot the values within the specific precipitation and elevation rasters shown
 594 have been used.

595

596



597

598 **Figure S3:** Tree species composition in the boreal zone of Mongolia and in the subunits of three
 599 different types of boreal forest. The tree species distribution was adapted from Data provided by
 600 NAMHEM, Ministry of Nature, Environment and Tourism, Mongolia (2009)

601

602 **References**

- 603 Academy of Sciences of Mongolia and Academy of Sciences of USSR: National Atlas of the Peoples
604 Republic of Mongolia, Ulan Baatar, Moscow, 144 pp., 1990.
- 605 Barthel, H.: Die regionale und jahreszeitliche Differenzierung des Klimas in der Mongolischen
606 Volksrepublik, *Studia geographica*, 34, 3–91, 1983.
- 607 Batima, P., Natsagdorj, L., Gombluudev, P., and Erdenetsetseg, B.: Observed climate change in
608 Mongolia, *AIACC Working Papers*, 12, 1–25, 2005.
- 609 Bat-Oyun, T., Shinoda, M., Cheng, Y., and Purevdorj, Y.: Effects of grazing and precipitation variability
610 on vegetation dynamics in a Mongolian dry steppe, *JPECOL*, 9, 508–519, doi:10.1093/jpe/rtv083,
611 2016.
- 612 Bayartaa, N., Goldammer, G., and Uibrig, H.: Fire situation in Mongolia, in: *International Forest Fire*
613 *News*, Goldammer, G. (Ed.), 36, 46–66, 2007.
- 614 Böhner, J.: General climatic controls and topoclimatic variations in Central and High Asia, *Boreas*, 35,
615 279–295, doi:10.1080/03009480500456073, 2006.
- 616 Busing, R. T. and Mailly, D.: Advances in spatial, individual-based modelling of forest dynamics, *J Veg*
617 *Sci*, 15, 831, doi:10.1658/1100-9233(2004)015[0831:AISIMO]2.0.CO;2, 2004.
- 618 Dashkhuu, D., Kim, J. P., Chun, J. A., and Lee, W.-S.: Long-term trends in daily temperature extremes
619 over Mongolia, *Weather and Climate Extremes*, 8, 26–33, doi:10.1016/j.wace.2014.11.003, 2015.
- 620 Dashtseren, A., Ishikawa, M., Iijima, Y., and Jambaljav, Y.: Temperature Regimes of the Active Layer
621 and Seasonally Frozen Ground under a Forest-Steppe Mosaic, Mongolia, *Permafrost and Periglac.*
622 *Process.*, 25, 295–306, doi:10.1002/ppp.1824, 2014.
- 623 Dee, D. P., Uppala, S. M., Simmons, A. J., Berrisford, P., Poli, P., Kobayashi, S., Andrae, U., Balmaseda,
624 M. A., Balsamo, G., Bauer, P., Bechtold, P., Beljaars, A. C. M., van de Berg, L., Bidlot, J., Bormann,
625 N., Delsol, C., Dragani, R., Fuentes, M., Geer, A. J., Haimberger, L., Healy, S. B., Hersbach, H.,
626 Hólm, E. V., Isaksen, I., Kållberg, P., Köhler, M., Matricardi, M., McNally, A. P., Monge-Sanz, B. M.,
627 Morcrette, J.-J., Park, B.-K., Peubey, C., Rosnay, P. de, Tavolato, C., Thépaut, J.-N., and Vitart, F.:
628 The ERA-Interim reanalysis: Configuration and performance of the data assimilation system,
629 *Q.J.R. Meteorol. Soc.*, 137, 553–597, doi:10.1002/qj.828, 2011.
- 630 Dorjsuren, C.: Anthropogenic succession in larch forests of Mongolia (in Russian), *Biological*
631 *Resources and Natural Conditions of Mongolia*, 1–260, 2009.
- 632 Dulamsuren, C.: Floristische Diversität, Vegetation und Standortbedingungen in der Gebirgstaiga des
633 Westkhentej, Nordmongolei, *Berichte des Forschungszentrums Waldökosysteme, Reihe A*, 191,
634 1–290, 2004.
- 635 Dulamsuren, C. and Hauck, M.: Spatial and seasonal variation of climate on steppe slopes of the
636 northern Mongolian mountain taiga, *Grassland Science*, 54, 217–230, doi:10.1111/j.1744-
637 697X.2008.00128.x, 2008.
- 638 Dulamsuren, C., Hauck, M., Bader, M., Osokhjargal, D., Oyungerel, S., Nyambayar, S., Runge, M., and
639 Leuschner, C.: Water relations and photosynthetic performance in *Larix sibirica* growing in the
640 forest-steppe ecotone of northern Mongolia, *Tree physiology*, 29, 99–110,
641 doi:10.1093/treephys/tpn008, 2009a.
- 642 Dulamsuren, C., Hauck, M., Bader, M., Oyungerel, S., Osokhjargal, D., Nyambayar, S., and Leuschner,
643 C.: The different strategies of *Pinus sylvestris* and *Larix sibirica* to deal with summer drought in a
644 northern Mongolian forest-steppe ecotone suggest a future superiority of pine in a warming
645 climate, *Can. J. For. Res.*, 39, 2520–2528, doi:10.1139/X09-156, 2009b.
- 646 Dulamsuren, C., Hauck, M., Khishigjargal, M., Leuschner, H. H., and Leuschner, C.: Diverging climate
647 trends in Mongolian taiga forests influence growth and regeneration of *Larix sibirica*, *Oecologia*,
648 163, 1091–1102, doi:10.1007/s00442-010-1689-y, 2010a.

649 Dulamsuren, C., Hauck, M., and Leuschner, C.: Recent drought stress leads to growth reductions in
650 *Larix sibirica* in the western Khentey, Mongolia, *Global change biology*, 16, 3024,
651 doi:10.1111/j.1365-2486.2009.02147.x, 2010b.

652 Dulamsuren, C., Hauck, M., and Mühlenberg, M.: Ground vegetation in the Mongolian taiga forest-
653 steppe ecotone does not offer evidence for the human origin of grasslands, *Appl Veg Sci*, 8, 149–
654 154, doi:10.1658/1402-2001(2005)008[0149:GVITMT]2.0.CO;2, 2005.

655 Dulamsuren, C., Khishigjargal, M., Leuschner, C., and Hauck, M.: Response of tree-ring width to
656 climate warming and selective logging in larch forests of the Mongolian Altai, *Journal of Plant
657 Ecology*, 7, 24–38, doi:10.1093/jpe/rtt019, 2014.

658 Dulamsuren, C., Klinge, M., Degener, J., Khishigjargal, M., Chenlemuge, T., Bat-Enerel, B., Yeruult, Y.,
659 Saindovdon, D., Ganbaatar, K., Tsogtbaatar, J., Leuschner, C., and Hauck, M.: Carbon pool
660 densities and a first estimate of the total carbon pool in the Mongolian forest-steppe, *Global
661 change biology*, 22, 830–844, doi:10.1111/gcb.13127, 2016.

662 Dulamsuren, C., Wommelsdorf, T., Zhao, F., Xue, Y., Zhumadilov, B. Z., Leuschner, C., and Hauck, M.:
663 Increased Summer Temperatures Reduce the Growth and Regeneration of *Larix sibirica* in
664 Southern Boreal Forests of Eastern Kazakhstan, *Ecosystems*, 16, 1536–1549, doi:10.1007/s10021-
665 013-9700-1, 2013.

666 Eckert, S., Hüsler, F., Liniger, H., and Hodel, E.: Trend analysis of MODIS NDVI time series for
667 detecting land degradation and regeneration in Mongolia, *Journal of Arid Environments*, 113, 16–
668 28, doi:10.1016/j.jaridenv.2014.09.001, 2015.

669 Erasmi, S., Schucknecht, A., Barbosa, M., and Matschullat, J.: Vegetation Greenness in Northeastern
670 Brazil and Its Relation to ENSO Warm Events, *Remote Sensing*, 6, 3041–3058,
671 doi:10.3390/rs6043041, 2014.

672 Giese, E., Mossig, I., Rybski, D., and Bunde, A.: Long-term analysis of air temperature trends in
673 Central Asia, *Erdkunde*, 61, 186–202, 2007.

674 Goldammer, G.: Fire Situation in Mongolia, in: *International Forest Fire News*, 26, 75–83, 2002.

675 Goldammer, G. (Ed.): *International Forest Fire News*, 36, 97 pp., 2007.

676 Gunin, P. and Vostokova, E.: *Ecosystems of Mongolia: Atlas*, Moscow, 48 pp., 2005.

677 Gunin, P. D., Vastokova, E. A., Dorofeyuj, N. I., Tarasov, P. E., and Black, C. C. (Eds.): *Vegetation
678 dynamics of Mongolia*, *Geobotany*, 26, Kluwer Academic Publishers, Dordrecht, Boston, London,
679 238 pp., 1999b.

680 Hais, M., Chytrý, M., and Horsák, M.: Exposure-related forest-steppe: A diverse landscape type
681 determined by topography and climate, *Journal of Arid Environments*, 135, 75–84,
682 doi:10.1016/j.jaridenv.2016.08.011, 2016.

683 Hansen, M. C., Potapov, P. V., Moore, R., Hancher, M., Turubanova, S. A., Tyukavina, A., Thau, D.,
684 Stehman, S. V., Goetz, S. J., Loveland, T. R., Kommareddy, A., Egorov, A., Chini, L., Justice, C. O.,
685 and Townshend, J. R. G.: High-resolution global maps of 21st-century forest cover change,
686 *Science (New York, N.Y.)*, 342, 850–853, doi:10.1126/science.1244693, 2013.

687 Harris, I., Jones, P. D., Osborn, T. J., and Lister, D. H.: Updated high-resolution grids of monthly
688 climatic observations - the CRU TS3.10 Dataset, *Int. J. Climatol.*, 34, 623–642,
689 doi:10.1002/joc.3711, 2014.

690 Hilbig, W.: *The vegetation of Mongolia*, SPB Acad. Publ., Amsterdam, 258 pp., 1995.

691 Holdridge, L.: Determination of world plant formations from simple climatic data, *Science*, 105, 367–
692 368, 1947.

693 Jobbágy, E. G. and Jackson, R. B.: Global controls of forest line elevation in the northern and southern
694 hemispheres, *Global Ecology & Biogeography*, 9, 253–268, 2000.

695 Karger, D. N., Conrad, O., Böhner, J., Kawohl, T., Kreft, H., Soria-Auza, R. W., Zimmermann, N., Linder,
696 H. P., and Kessler, M.: Climatologies at high resolution for the earth's land surface areas,
697 arXiv:1607.00217 [physics.ao-ph], 1–20, 2016.

698 Karger, D. N., Conrad, O., Böhner, J., Kawohl, T., Kreft, H., Soria-Auza, R. W., Zimmermann, N. E.,
699 Linder, H. P., and Kessler, M.: Climatologies at high resolution for the earth's land surface areas,
700 *Scientific data*, 4, 170122, doi:10.1038/sdata.2017.122, 2017.

701 Khansaritoreh, E., Dulamsuren, C., Klinge, M., Ariunbaatar, T., Bat-Enerel, B., Batsaikhan, G.,
702 Ganbaatar, K., Saindovdon, D., Yeruult, Y., Tsogtbaatar, J., Tuya, D., Leuschner, C., and Hauck, M.:
703 Higher climate warming sensitivity of Siberian larch in small than large forest islands in the
704 fragmented Mongolian forest steppe, *Global change biology*, doi:10.1111/gcb.13750, 2017.

705 Klinge, M.: Glazialgeomorphologische Untersuchungen im Mongolischen Altai als Beitrag zur
706 jungquartären Landschafts- und Klimageschichte der Westmongolei, *Aachener Geographische*
707 *Arbeiten*, 35, Aachen, 125 pp., 2001.

708 Klinge, M., Böhner, J., and Erasmi, S.: Modeling forest lines and forest distribution patterns with
709 remote-sensing data in a mountainous region of semiarid central Asia, *Biogeosciences*, 12, 2893–
710 2905, doi:10.5194/bg-12-2893-2015, 2015.

711 Klinge, M., Böhner, J., and Lehmkuhl, F.: Climate patterns, snow- and timberlines in the Altai
712 Mountains, Central Asia, *Erdkunde*, 57, 296–308, 2003.

713 Körner, C.: *Alpine treelines: Functional ecology of the global high elevation tree limits*, Springer, Basel
714 [u.a.], 220 pp., 2012.

715 Körner, C. and Paulsen, J.: A world-wide study of high altitude treeline temperatures, *Journal of*
716 *Biogeography*, 31, 713–732, doi:10.1111/j.1365-2699.2003.01043.x, 2004.

717 Liu, H., Park Williams, A., Allen, C. D., Guo, D., Wu, X., Anenkhonov, O. A., Liang, E., Sandanov, D. V.,
718 Yin, Y., Qi, Z., and Badmaeva, N. K.: Rapid warming accelerates tree growth decline in semi-arid
719 forests of Inner Asia, *Global change biology*, 19, 2500–2510, doi:10.1111/gcb.12217, 2013.

720 Lu, D., Chen, Q., Wang, G., Liu, L., Li, G., and Moran, E.: A survey of remote sensing-based
721 aboveground biomass estimation methods in forest ecosystems, *International Journal of Digital*
722 *Earth*, 9, 63–105, doi:10.1080/17538947.2014.990526, 2014.

723 Miao, L., Liu, Q., Fraser, R., He, B., and Cui, X.: Shifts in vegetation growth in response to multiple
724 factors on the Mongolian Plateau from 1982 to 2011, *Physics and Chemistry of the Earth, Parts*
725 *A/B/C*, 87-88, 50–59, doi:10.1016/j.pce.2015.07.010, 2015.

726 Mieke, G., Mieke, S., Koch, K., and Will, M.: *Sacred Forests in Tibet*, *Mountain Research and*
727 *Development*, 23, 324–328, doi:10.1659/0276-4741(2003)023[0324:SFIT]2.0.CO;2, 2003.

728 Ministry of the Environment Japan: *Climate change in Mongolia: Output from GCM*, 12 pp., 2015.

729 Murzaev, E. M.: *Die Mongolische Volksrepublik. - Physisch-geographische Beschreibung*, Gotha, 521
730 pp., 1954.

731 Paulsen, J. and Körner, C.: A climate-based model to predict potential treeline position around the
732 globe, *Alp Botany*, 124, 1–12, doi:10.1007/s00035-014-0124-0, 2014.

733 Poulter, B., Pederson, N., Liu, H., Zhu, Z., D'Arrigo, R., Ciais, P., Davi, N., Frank, D., Leland, C., Myneni,
734 R., Piao, S., and Wang, T.: Recent trends in Inner Asian forest dynamics to temperature and
735 precipitation indicate high sensitivity to climate change, *Agricultural and Forest Meteorology*,
736 178-179, 31–45, doi:10.1016/j.agrformet.2012.12.006, 2013.

737 Sato, T., Kimura, F., and Kitoh, A.: Projection of global warming onto regional precipitation over
738 Mongolia using a regional climate model, *Journal of Hydrology*, 333, 144–154,
739 doi:10.1016/j.jhydrol.2006.07.023, 2007.

740 Schlütz, F., Dulamsuren, C., Wieckowska, M., Mühlenberg, M., and Hauck, M.: Late Holocene
741 vegetation history suggests natural origin of steppes in the northern Mongolian mountain taiga,

742 Palaeogeography, Palaeoclimatology, Palaeoecology, 261, 203–217,
743 doi:10.1016/j.palaeo.2007.12.012, 2008.

744 Sharkhuu, A., Sharkhuu, N., Etzelmüller, B., Heggem, E. S. F., Nelson, F. E., Shiklomanov, N. I.,
745 Goulden, C. E., and Brown, J.: Permafrost monitoring in the Hovsgol mountain region, Mongolia,
746 J. Geophys. Res., 112, doi:10.1029/2006JF000543, 2007.

747 Sharkhuu, N.: Recent changes in the permafrost of Mongolia, in: Proc. 8th Int. Conf. Permafrost, 21–
748 25 July 2003, Zurich, Switzerland, M. Phillips, S. M. Springman, and L. U. Arenson (Ed.), Zurich,
749 Switzerland, 21-25 July 2003, Swets & Zeitlinger, Lisse, Netherlands, 2003.

750 Sugimoto, A., Yanagisawa, N., Naito, D., Fujita, N., and Maximov, T. C.: Importance of permafrost as a
751 source of water for plants in east Siberian taiga, Ecol Res, 17, 493–503, doi:10.1046/j.1440-
752 1703.2002.00506.x, 2002.

753 Szumińska, D.: Changes in surface area of the Böön Tsagaan and Orog lakes (Mongolia, Valley of the
754 Lakes, 1974–2013) compared to climate and permafrost changes, Sedimentary Geology, 340, 62–
755 73, doi:10.1016/j.sedgeo.2016.03.002, 2016.

756 Treter, U.: Gebirgs-Waldsteppe in der Mongolei, Geographische Rundschau, 48, 655–661, 1996.

757 Tsogtbaatar, J.: Deforestation and reforestation needs in Mongolia, Forest Ecology and Management,
758 201, 57–63, doi:10.1016/j.foreco.2004.06.011, 2004.

759 Vandandorj, S., Gantsetseg, B., and Boldgiv, B.: Spatial and temporal variability in vegetation cover of
760 Mongolia and its implications, J. Arid Land, 7, 450–461, doi:10.1007/s40333-015-0001-8, 2015.

761 Walter, H. and Breckle, S.-W.: Spezielle Ökologie der gemäßigten und arktischen Zonen Euro-
762 Nordasiens: Zonobiom VI - IX ; 232 Tabellen, 2., überarb. Aufl., UTB für Wissenschaft Große
763 Reihe, Geo-Biosphäre / Heinrich Walter; Siegmund-W. Breckle ; Bd. 3, Fischer, Stuttgart, 726 pp.,
764 1994.

765 Watson, D.: Contouring: A Guide to the Analysis and Display of Spatial Data, Computer methods in
766 the Geosciences, 10, Pergamon Press, London, 204 pp., 1992.